PROBABILISTIC SEISMIC VULNERABILITY ANALYSIS OF REINFORCED CONCRETE COLUMNS

VLAD CEANGU , DAN CRETU

Abstract. Estimating the response of reinforced concrete columns to a transitory action, represented by a ground motion, is an uncertain task. The randomness of the seismic event and that of the response should be accounted for. The probabilistic seismic vulnerability analysis is a method that one can use for estimating confidence intervals for the response of reinforced columns. In this paper a mixed method using numerical analysis results coupled with experimental data is used for the assessment of the vulnerability of reinforced concrete columns.

Key words: performance based earthquake engineering, vulnerability of reinforced concrete columns, seismic demand analysis, ductility of reinforced concrete columns.

1. INTRODUCTION

In earthquake engineering the assessment of the response of reinforced concrete columns suppose that at different limit states, which have a particular damage measure *DM*, a mean annual frequency of exceedance is associated. These limit states are chosen as different observable events for the behavior of reinforced concrete columns at a cyclic action [5]. Each limit state has a particular description and an associated intervention cost. The mean annual frequency of the necessary intervention cost is an output of the performance based earthquake engineering procedure.

The limit states used for approximating the vulnerability of reinforced concrete columns are of two categories, according to including or not the collapse of the specimen. The description of these limit states is found in experimental reports or data-bases of such reports. In this paper the data-base used is that presented in [1], using the data for the rectangular columns, with some replacements and adjustments from [3]. The total number of columns used is 272 with the following described limit states: (1) crushing of concrete cover, (2) spalling of concrete cover, (3) buckling of longitudinal reinforcement, (4) rupture of longitudinal reinforcement, (5) rupture

Technical University of Civil Engineering Bucharest, Romania

of transversal reinforcement, (6) loss of axial strength and (7) element failure. The first three limit states are non-collapse states, the rest have associated the element failure (7) state. It is noted that not all columns presented in the data-base have these limit states noted or observed, and in some cases geometrical or material data is missing.

For each column used from the data-base a force-displacement experiment data-file is provided. The cyclic displacement is that of a cantilever column with an axial load applied at the top. The data is transformed for columns with other configurations. Second-order effects are not included to the force-displacement data. The cyclic action is applied at a particular point on the height of the column, and the measured or the effective length of the column is determined from that point to the fixed base. The associated ductility, the hysteretic dissipated energy and other parameters are approximated using the available experimental data.

Using the parameters from the data-base and a numerical model, a fragility curve is approximated for each limit state. The fragility curve developed in this paper represent the variability observed from the experiments for one particular limit state and that of the numerical model used to approximate the particular limit state. The mean annual frequency of exceedance of one particular limit state is as follows:

$$\lambda_{DM} = \int P[\text{DM} > y \,|\, \text{EDP} = z] \, \mathrm{d}\lambda_{EDP}(z) \qquad (1)$$

where $P[\text{DM} > y \,|\, \text{EDP} = z]$ is the fragility curve expressed as the probability of a damage measure DM exceeding a particular value y when an engineering demand parameter EDP is equal to the value z associated to one limit state. The second term $\mathrm{d}\lambda_{EDP}(z)$ is the differential variation of the mean annual frequency of exceedance in point z approximated by using the probabilistic seismic demand analysis PSDA [13]. This quantity is estimated based on the values of intensity seismic measures from a probabilistic hazard analysis and is approximated using the following equation:

$$\lambda_{EDP} = \int P[\text{EDP} > z \,|\, \text{IM} = \text{im}] \, \mathrm{d}\lambda_{IM} \qquad (2)$$

where $P[\text{EDP} > z \,|\, \text{IM} = \text{im}]$ is the probability of an engineering demand parameter to exceed some value given an intensity measure IM equal to a particular *im* value. This term is approximated by using methods of structural engineering such as incremental dynamic analysis [15] or those based on selection of appropriate ground motions [13]. The second term $\mathrm{d}\lambda_{IM}$ is the differential variation of the seismic hazard curve approximated for the equivalent linear single degree of freedom system with period *T*.

Equation (1) is generally numerically solved as a function of the seismic intensity measure IM and the damage measure hazard curve DMHC is approximated by using the following form [7]:

$$\lambda_{DM} = \lambda_{M_{w,\min}} \sum_i \sum_j \sum_k P[\mathrm{DM} > \mathrm{dm}_i \,|\, \mathrm{DM} = \mathrm{dm}_i] \, P[\mathrm{DM} = \mathrm{dm}_i \,|\, \mathrm{EDP} = \mathrm{edp}_j]$$

$$P[\mathrm{EDP} = \mathrm{edp}_j \,|\, \mathrm{IM} = \mathrm{im}_k] \, P[\mathrm{IM} = \mathrm{im}_k]. \qquad (3)$$

The first right term of equation (3), $\lambda_{M_{w,\min}}$, is the mean annual frequency of earthquakes with a magnitude chosen equal to the minimum one [10].

To evaluate the vulnerability of reinforced concrete columns, three particular procedures are followed. The first is the probabilistic seismic analysis PSHA which approximates IM values from a seismic hazard curve SHC, the second is the probabilistic seismic demand PSDA analysis which approximates EDP values from a seismic demand hazard curve SDHC using the results from PSHA analysis and the third is the probabilistic seismic vulnerability analysis PSVA which approximates DM values from a damage measure hazard curve DMHC. The vulnerability of reinforced concrete columns is expressed as the mean annual frequency of exceeding a given limit state.

2. DATA-BASE OF REINFORCED CONCRETE COLUMNS

The concrete columns available in the data-base have different geometry, type and reinforcement ratios, loading conditions and general behavior. The majority of these columns have a flexural type failure with softening behavior after the peak force and all columns have transverse reinforcement. The concrete used for the columns is normal or high strength concrete, with ductile reinforcement. The values of the yield strength and ultimate strength of the used materials are provided by the authors of the experiments, and as mentioned earlier some values are missing. In the following table, general information about the geometry, materials and general type of columns used are presented.

Table 1
General information for the rectangular concrete columns

	Mean	Standard deviation	Covariance	P-Δ	1	2	3	4
					76	137	50	7
L [mm]	1086	530	0.488	Config.	C	DC		DE
h [mm]	320	122	0.381		104	85		83
f_c [MPa]	51	28.6	0.561	Failure Type	Flexure	Shear		F-S
f_{ybl} [MPa]	434	59	0.136		209	23		40
f_{yew} [MPa]	483	215	0.445	ρ_l [%]	Mean	Std.		Cov.
					2.767	1.197		0.432
n	0.258	0.196	0.760	ρ_{ew} [%]	Mean	Std.		Cov.
					0.794	0.5		0.631

The abbreviations of the configuration types have the meaning of C – cantilever, DC – double cantilever, DE – double ended (clamped at both ends). The types of P-Δ configurations are consistent with the way the vertical and lateral load are applied [1], types one and two correspond to the cases when the effective horizontal force is computed from the second order effects, or as the one given by the authors of experiments in the second case.

There are eight types of confinement configurations, usually one rectangular tie around the perimeter with or without supplemental ties arranged in different ways. The number of ties on each face is given in the data-base and so the compressive strength and ultimate strain of confined concrete is approximated using two models, the model from [9] for normal concrete and the model from [6] for high strength concrete.

Using the force-displacement text files given for each experiment the normalized hysteretic energy is approximated as the ratio between the dissipated energy in one complete cycle to that of the corresponding perfect plastic model in one cycle. For each column the area from the reported cyclic loops is computed and based on the maximum and minimum cycle force and displacement the area of the loop of the perfect plastic model is approximated.

To estimate the ductility of the columns an approximate procedure is used based on the usage of backbone curves. These backbone curves are approximated fitting the following equations on the force-displacement data for each column:

$$f/f_{max} = \theta_1 \left[1 - \left(1 - d/d_{max} \right)^{\theta_2} \right], \quad d \leq d_{max}$$

$$f/f_{max} = 1 \big/ \left[1 + \theta_3 \left(d/d_{max} \right)^{\theta_4} \right], \quad d \leq d_{ul}, \tag{4}$$

where θ_i are coefficients evaluated by nonlinear regression, d_{max} is the displacement associated with the maximum observed force and d_{ul} is the displacement recorded in the last cycle, considered as the maximum allowable displacement if it is not reported by the authors of the experiment.
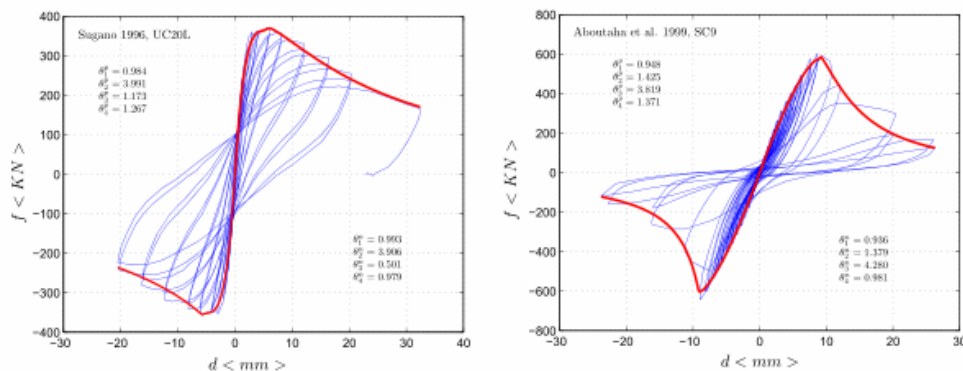

Fig. 1 – Backbone curves of two reinforced concrete columns.

Using equation (4) and the force – displacement data of two columns from the database, the backbone curves from Fig. 1 are approximated. These curves are representative as a monotonic incremental load applied at the end of the cantilever versus the measured displacement. The two intervals of equation (4) are a function of $f_{\max}$ and so three modes of plastic behavior can be considered: hardening, approximately elasto-perfect-plastic and softening. In Fig. 1 only the softening behavior is plotted.
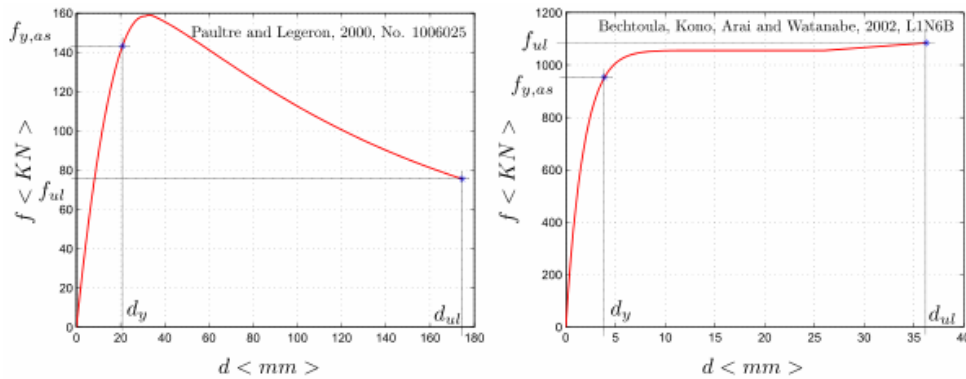

Fig. 2 – Characteristic yield point.

In Fig. 2 the used characteristic yield point is represented. Based on the backbone curves of the force-displacement data, an equivalent yield point is chosen as the drop of lateral stiffness of 90%. Effectively the yield displacement corresponding to the point when the ratio of the effective tangent stiffness and the initial tangent stiffness is less than 10%, where the tangent stiffness $k_{\text{tg},i} = (\partial f / \partial d)_i$ is evaluated using equation (4). Based on this point, an effective yield moment and displacement is approximated.

From the above procedure for each column the dissipated hysteretic normalized energy $E_{h,\text{norm}}$ and the equivalently observed maximum attained ductility μ_c are approximated. These two parameters are considered response parameters as engineering demand parameters EDP, in Table 2 the coefficient of correlation between these parameters and some of the input variables are given.

Table 2

Correlation coefficients between the response parameters μ_c, $E_{h,\text{norm}}$ and the column parameters

	L/h	f_c	α_s	ρ_l	ρ_{ew}	n	k_{conf}	μ	$E_{h,\text{norm}}$
μ_c	0.122	0.172	−0.043	−0.081	0.265	0.039	0.372	1.000	0.305
$E_{h,\text{norm}}$	0.197	0.135	−0.373	0.277	0.298	0.098	0.248	0.305	1.000

The input variables in percentages used are: α_s for the reinforcement steel, the transversal and longitudinal reinforcement ratios ρ_{ew} and ρ_l, the normalized axial force n, the confinement efficiency factor k_{conf} defined as the ratio of maximum stress of the confined concrete to the unconfined one, the concrete characteristic strength f_c and the shear span to section height ratio L/h. In the following two figures the correlation between some of the input parameters, the response factors and the observed type of failure is plotted [3].
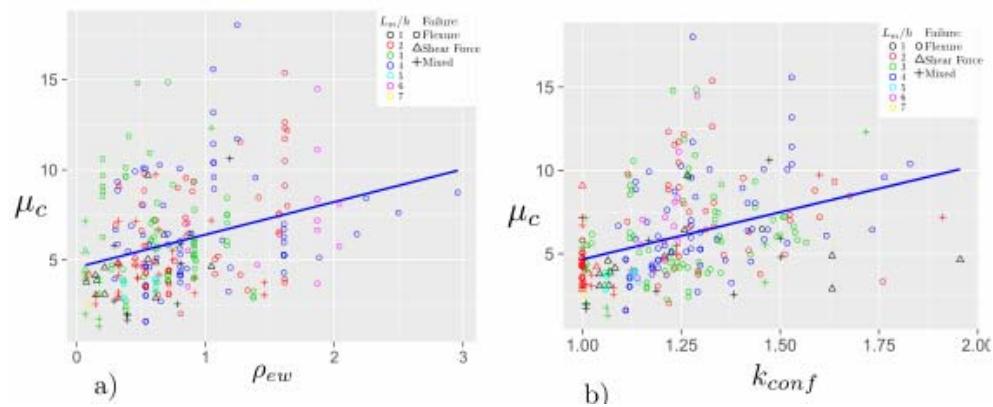
Fig. 3 – Maximum ductility μ_c as a function of: a) transverse reinforcement ratio ρ_{ew};
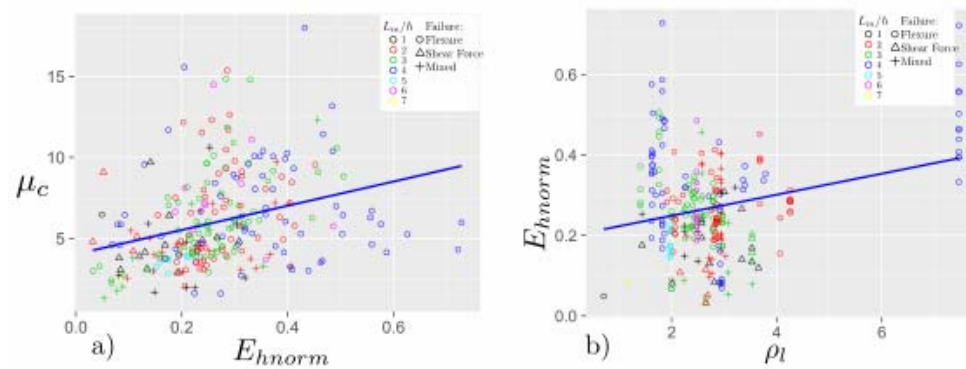b) confinement efficiency coefficient k_{conf}.

Fig. 4 – a) Maximum ductility μ_c as a function of normalized hysteretic energy $E_{h,\,norm}$;
b) normalized hysteretic energy $E_{h,\,norm}$ as a function of the longitudinal reinforcement ratio ρ_l.

From Fig. 3, it is observed that the estimated ductility of reinforced concrete columns is increasing as the transversal reinforcement ratio ρ_{ew} and the confinement efficiency coefficient k_{conf} increases. For short elements, the values approximated

tend to be smaller than the mean values and the majority of these elements have a shear failure type. Generally, elements that exhibit mixed or shear failure type have lower values of transverse reinforcement ratios and confinement efficiency coefficients. Nonetheless, for some elements with mixed or shear failure type high ductility values are observed. Figure 4a shows that the approximated ductility increases as the normalized hysteretic energy is increasing and that the shear and mixed failure modes have the smaller values of the ductility and normalized hysteretic energy. Figure 4b shows that the approximated normalized hysteretic energy is a function of the ratio of longitudinal reinforcement ρ_l also.

With the geometrical characteristics and material properties given or computed based on data given in the data-base, an numerical model is assembled for approximating engineering demand parameters.

The finite element model used for the columns is the force-based beam-column element [12, 14] coupled with hinges for the interaction of bending moment with shear force or/and axial force [5, 8], strain penetration material models and loss of anchorage or buckling [17]. These elements are implemented in the *Open Sees* framework [11]. The fiber sections mesh dimensions and the number of interpolation points used are those recommended in [2].

The type of analysis employed is the transient analysis with the displacements from experiment applied at the top node of each numerical model of the column. The same displacements, but other forces and hysteretic energy will be obtained. The results from the numerical analysis compared to that approximated from the experimental data are plotted in Fig. 5 for two numerical models. The first model considers that the concrete constitutive law without tension strength, the second model considers it with tension strength and both models do not account for the shear-flexure interaction.
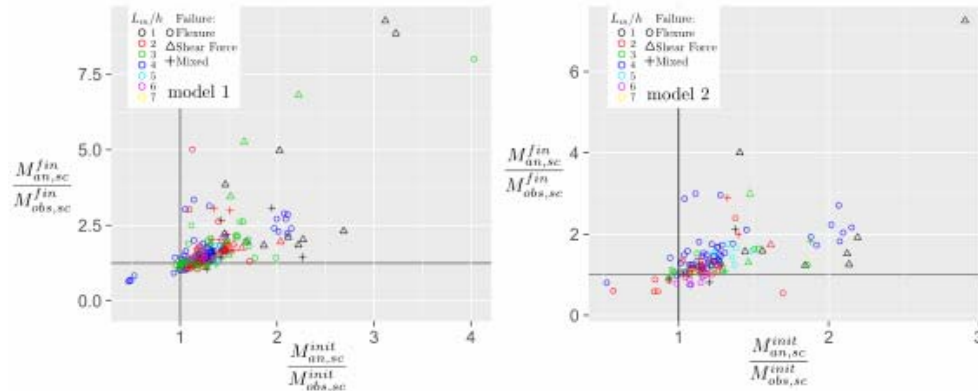

Fig. 5 – Ratio between the numerical approximated bending moment and experimental results for initial and final cycles as function of the maximum force for: a) model 1; b) model 2.

It is observed in Fig. 5 that the mean values of the ratios between the numerical approximated and experimental results are 1.26 for flexural failure and

1.40 for mixed failure. For shear failure the mean ratio is 1.90. Using the interaction hinge for shear-bending component, the mean ratio decreases to 1.43. The limit states mentioned in the first section will be numerically evaluated using the displacements corresponding to the strains associated to these limit states [2, 4].

The results obtained as ratios from the experimental given data are plotted in Figs. 6 and 7. These represent limit states are showed only for specimens that had these limit states reported.

These reported limit states have different influence in the behavior of columns at cyclic action. One column has multiple consecutive limit states before collapsing, or it exhibits at collapse only one type of limit state or a combined state. This is a function of the failure model. If a specimen has a flexure type failure, then it can exhibit multiple limit states. If the specimen has a shear type failure then, generally, it exhibits only one or few limit states.
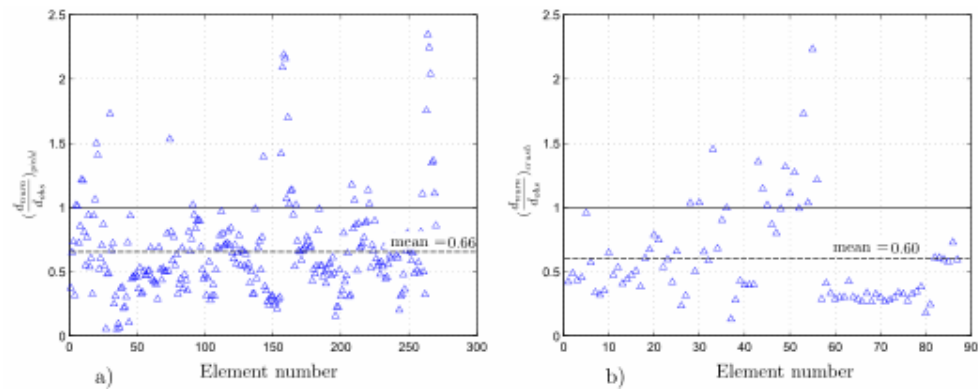

Fig. 6 – Ratios for: a) approximate yield (272 points);
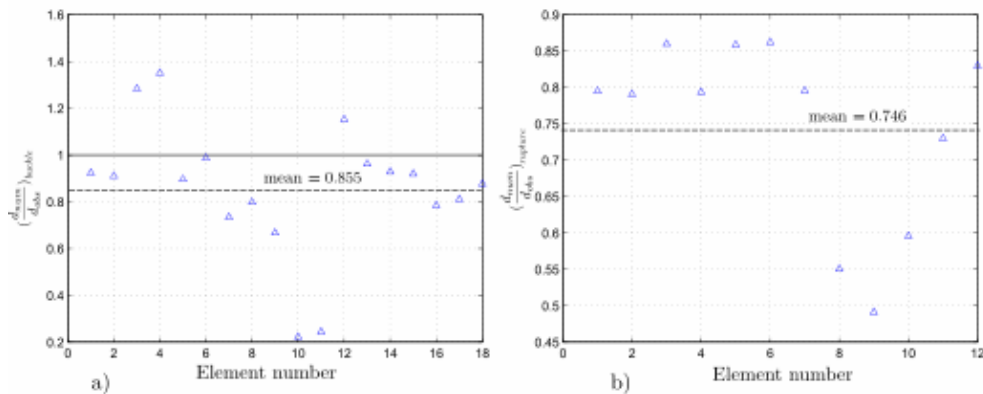b) crush of concrete cover (105 points).

Fig. 7 – Ratios for: a) buckling of longitudinal reinforcement (16 points);
b) rupture of longitudinal reinforcement (11 points).

3. FRAGILITY CURVES

Using a mixed method based on the results in the previous section, fragility curves are approximated for five reported limit states of the reinforced concrete columns. Fragility curves are cumulative distribution functions $F_{DM}(\text{dm})$ of a particular damage measure.

To fully define fragility curves, a mean and a standard deviation is approximated. The empiric cumulative distributions of the ratios of numerical estimated ductility to the approximated experimental one is conditioned on the number of available data. The fragility functions used herein describe the aleatory observations of different limit states and the differences observed for the numerical model used.

For each DM the empiric cumulative distribution is approximated using the available data and if the data is missing then is considered null because the numeric model doesn't reach that limit state and the collapse is obtained at a different state. Three types of distribution are tested, namely the normal, log-normal and Weibull distributions. The quantitative test for estimation criteria is Kolmogorov-Smirnov with the critical coefficient as a function of the number of data pairs. In Figure 8a the results obtained are presented with their particular critical values.

The values chosen for the critical coefficient $D_{2,cr}$ are for a confidence factor of 95%. As it is observed, the log-normal distribution has the lowest D_2 coefficients. The coefficient of variation using the log-normal distribution for each limit state are: $\text{Var}_{crush} = 40.9\%$, $\text{Var}_{buc} = 12.6\%$, $\text{Var}_{rup} = 21.2\%$ and $\text{Var}_{r,ew} = 50.8\%$. The ultimate limit state of ties and that of crushing of concrete cover are the most uncertain states.

These curves represent the first term of equation (1) written as follows:

$$P[\text{DM} > \text{dm} \,|\, \text{EDP} = z] = 1 - \Phi\left(\frac{\ln \text{dm} - \text{mean}_{\ln DM}}{sd_{\ln DM}}\right) \tag{5}$$

with the mean and standard deviation approximated from each of the fragility curve from Fig. 8 for different values of the damage measure.

Reinforced concrete columns can have collapse which is achieved at a particular limit state. The probability of appearance of a limit state $P(\text{LS})$ is equal to the number of observations of that limit state from the total number of observations.

The complete fragility model is obtained considering the probability that the expected ductility is equal to that associated with the ductility of the limit state and the expected one expressed as the multivariate distribution $P[\text{DM} = \text{dm}, \text{EDP} = \text{edp}]$. This distribution is obtained as the product of the distribution of DM, $P[\text{DM} = \text{dm} \,|\, \text{EDP}_{SL} = \text{edp}]$, and the distribution of EDP at a particular limit state

$P[\text{EDP} = \text{edp}]$. The sum of this joint distribution is almost equal to one and it can be obtained for each limit state. In Fig. 9 an example of two distributions is given. It is observed that the variability considered for the limit state is less than that of $\text{EDP}_{SL} = \text{edp}$.
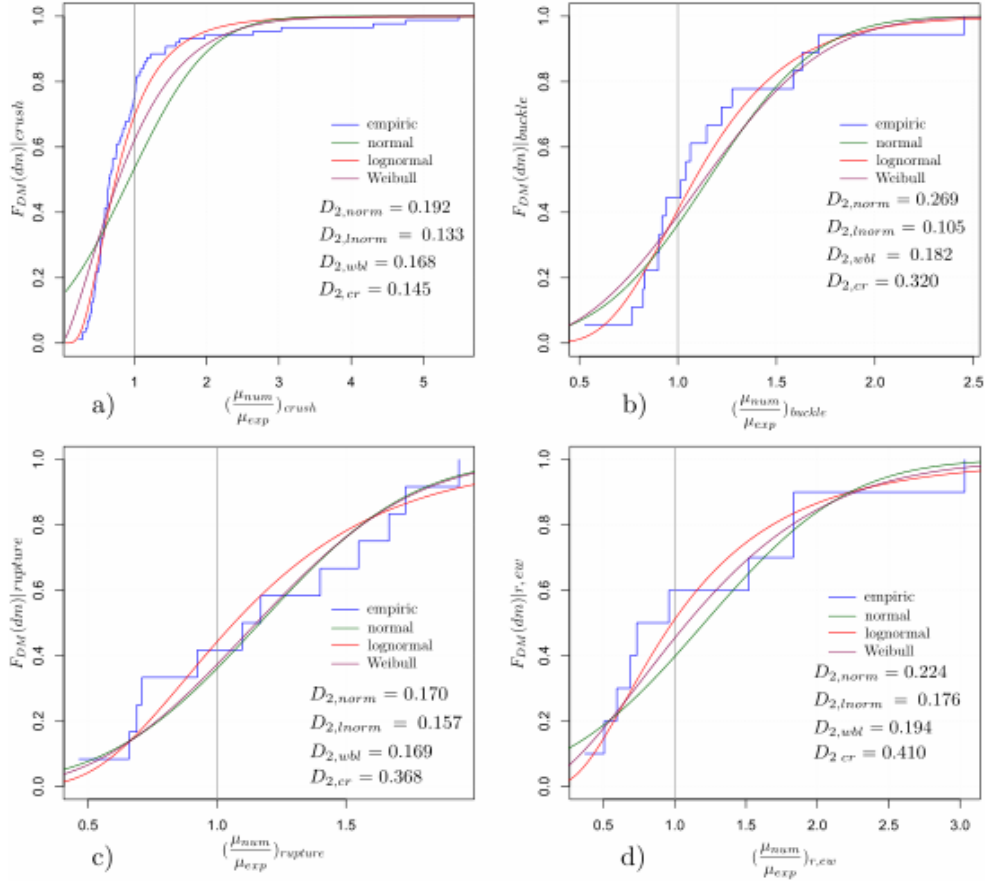

Fig. 8 – Fragility curves for: a) crushing of concrete cover; b) buckling of longitudinal reinforcement; c) rupture of longitudinal reinforcement; d) rupture of ties.

The observed limit states in the joint distribution $P[\text{DM} = \text{dm} \mid \text{EDP}_{SL} = \text{edp}]$ are included in the form:

$$P[\text{DM} = \text{dm} \mid \text{EDP}_{SL}] = (1 - P[\text{SL}]) P[\text{DM} = \text{dm} \mid \text{EDP}_{SL}, \text{nSL}] + $$
$$+ P[\text{SL}] P[\text{DM} = \text{dm} \mid \text{EDP}_{SL}, \text{SL}], \tag{6}$$

where $P[\text{DM} = \text{dm} \mid \text{EDP}_{SL}, \text{nSL}]$ if the probability that DM is equal to a particular value when EDP is not equal to EDP_{SL} – the value associated to a particular limit state.
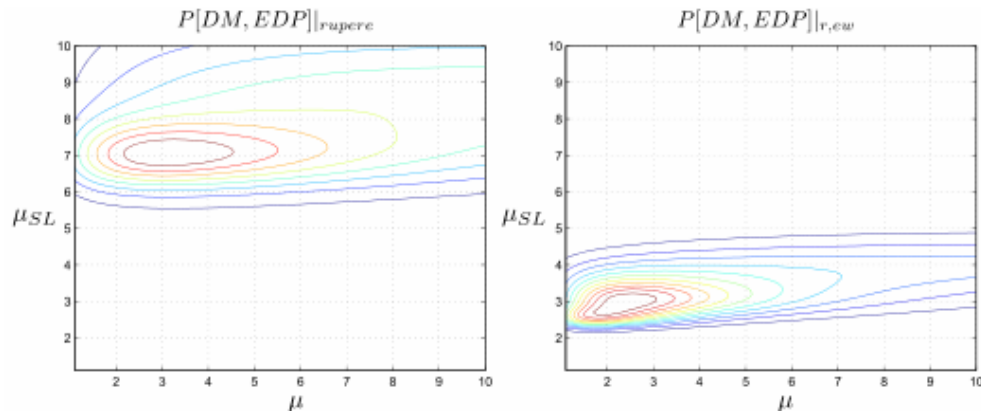
Fig. 9 – Joint log-normal distribution of $P[\text{DM}, \text{EDP}]$.

4. PROBABILISTIC SEISMIC VULNERABILITY ANALYSIS

To approximate the mean annual frequency of exceedance of an particular DM value it is necessary to evaluate the mean rate of occurrence of EDP values. This procedure is called probabilistic seismic demand analysis (PSDA) and is solved by using equation (2) and the numerical model presented in the section above. Engineering demand parameters are estimated using values from a seismic demand hazard curve SDHC.

4.1. Seismic action

The method for selecting ground motions used herein is based on the condition that the elastic and inelastic spectra of the selected records to be similar to that of the spectra of the accelerogram recorded at the INCERC station in 04.03.1977 after the Vrancea event. These records are selected from the *ROMPLUS* and *PEER* data-base and in total a number of 15 accelerograms are chosen. These used ground motions have the property that the frequency content is similar to that of the selected reference one. These accelerograms are scaled linearly to different hazard levels corresponding to a seismic hazard curve.

The seismic hazard curve is obtained using a probabilistic seismic hazard analysis with the Cornell-Mcguire method [10] for a fictitious site, situated at 100 km from the Vrancea source on a soft soil site, with intensity measures approximated using the ground motion model proposed by [16]. The derivate of the hazard curve is obtained using the format proposed by Kennedy and Short [7]. In Fig. 10, the elastic spectra of the accelerograms and a typical hazard curve and its derivate is plotted.
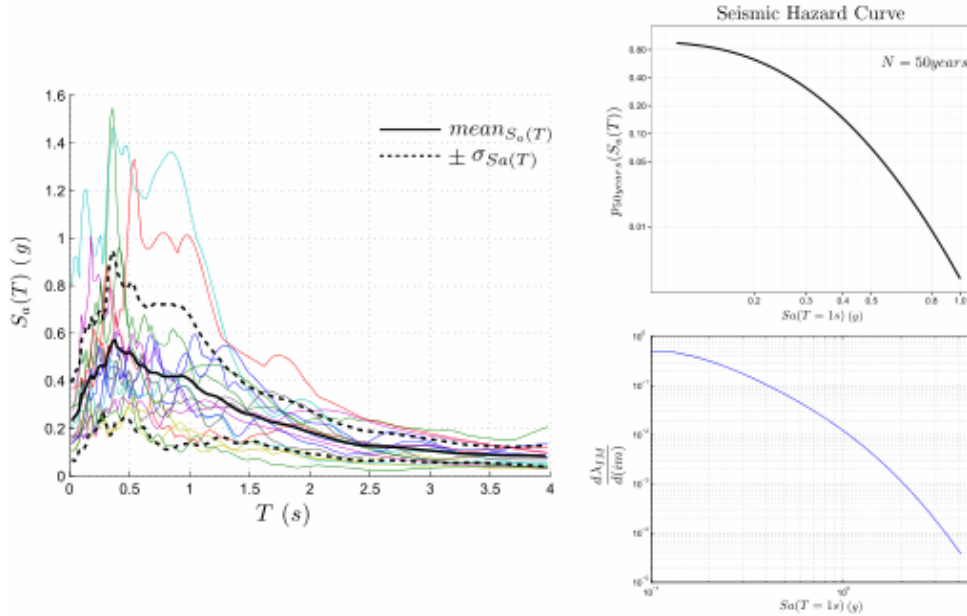
Fig. 10 – Elastic spectra of used accelerograms and the seismic hazard curve and its derivate.

4.2. Probabilistic Seismic Demand Analysis

With the information in the previous subsection and using equation (2), the mean annual frequency of exceedance of an engineering demand parameter is estimated. The only unknown quantity is the first term of equation (2), which is approximated using the incremental dynamic analysis [15]. Using the nonlinear mathematical model of the reinforced concrete columns for each accelerogram at each scale factor, a nonlinear dynamic analysis is completed and individual response parameters are obtained. After interpolating the results, a functional is used to approximate the response as a function of IM and the IDA curve is obtained.

Each point on the IDA curve represents the mean value of $\ln \text{IM}$ and at this point a particular standard deviation $\sigma_{\ln IM}$ is approximated. A log-normal distribution of a given mean and standard deviation can be given to the values of EDP as a function of IM, $P[\text{EDP} > z \mid \text{IM} = \text{im}]$. In Fig. 11 the IDA curve and the seismic demand hazard curve are represented.

The seismic demand hazard curve represents the mean annual frequency of exceedance of a particular EDP value for a system exposed to the seismic hazard associated to Vrancea source. These factors have no collapse included and the behavior is not corrected to that of a real system. This kind of analysis gives informations about the numerical response of the chosen type of modeling. In the probabilistic seismic vulnerability analysis the first derivative of λ_{EDP} will be approximated by central finite differences.
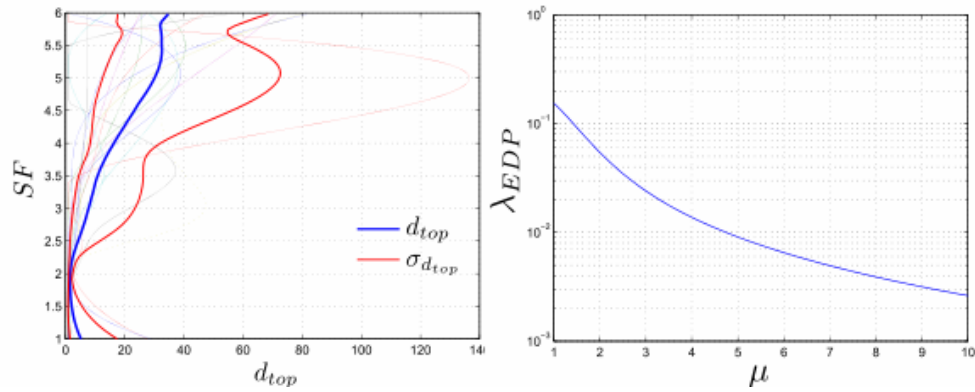
Fig. 11 – IDA curve and the seismic demand hazard curve SDHC.

4.3. Assessing vulnerability

Using the results from the PSDA analysis, the fragility curves approximated earlier and the total probability theory from equation (1), the mean annual frequency of exceedance of a particular limit state is evaluated. Equation (3) is written in a simplified form as:

$$\lambda_{DM} = \sum_{i=1}^{i=m} P[\text{DM} > \text{dm} \mid \text{EDP} = z_i] \cdot \frac{\text{d}\lambda_{EDP}}{\text{d}z} \mid_{z_i}. \tag{7}$$

A number of four columns are chosen from the data-base, with equivalent elastic periods of 0.30 s, 0.50 s, 0.80 s and 1.00 s. All these columns exhibit flexural failure and those with periods of 0.30 s and 0.50 s are stiffer than the other two and have a higher lateral strength. In Fig. 12 the DMHC curves are plotted.

a)   b)
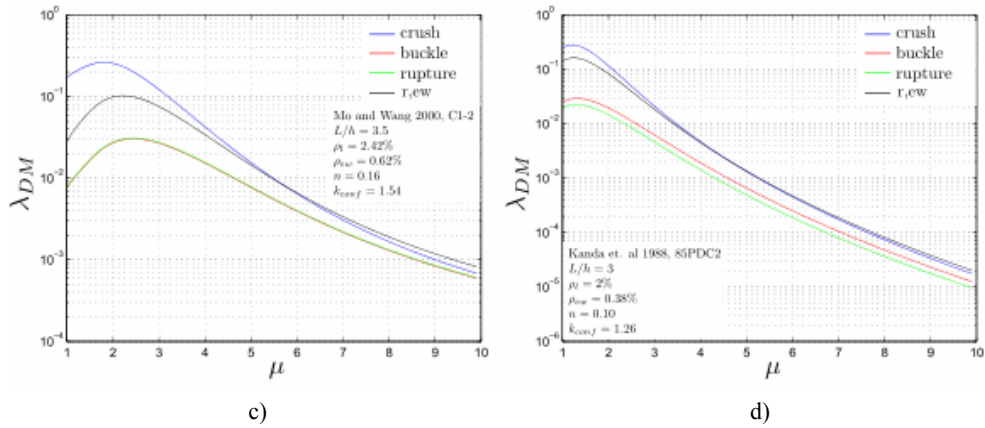
c)   d)
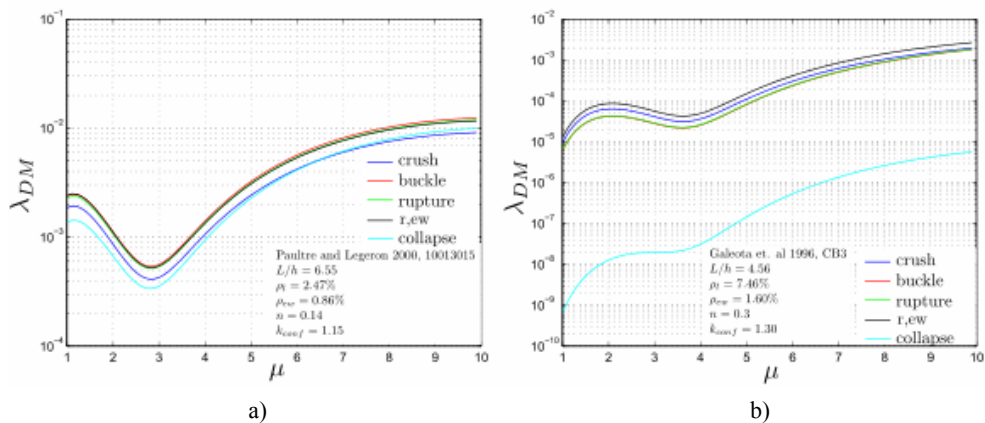
Fig. 12 – DMHC curves for four chosen columns from the data-base
with equivalent elastic periods: a) 0.8 s; b) 1.0 s; c) 0.3 s; d) 0.5 s.

It is observed that these distributions are a function of the EDP values, at each limit state λ_{DM} is a function of the appearance of a particular EDP value. This value has a recurrence interval for the DM values. In the case of weak systems there is no distinction between limit states; the collapse is the reported limit states almost in all cases. For either level of the scaling factors the model will give approximate values in almost all limit states. In the case of rigid systems the observed limit states are different for each scaling interval, so such model could represent the consecutive development of limit states.

The vulnerability assessment is defined as the mean frequency of exceedance λ_{DM}. The values associated to a particular level of hazard are approximated using the values evaluated in the numerical analysis for each limit state. The values on these curves are defined as local points associated to a limit state.

5. CONCLUSIONS

The required steps of the probabilistic seismic vulnerability analysis are given in this paper. The procedure is based on results evaluated using the probabilistic seismic hazard analysis and the probabilistic seismic demand analysis. These two procedures are independent of the vulnerability analysis but are interdependent. The PSDA analysis requires data from the PSHA analysis.

In the vulnerability assessment the probability of exceedance of a particular value of damage measure is evaluated. This probability is associated to an intensity measure or an engineering demand parameter. Using the damage measure hazard curve the expected damage in a period of time can be estimated or the mean

interval of recurrence, $1/\lambda_{DM}$, for a particular limit state can be approximated. Generally, a greater intensity measure means greater expected damage.

This procedure associates for the engineering demand parameter a quantity to evaluate with confidence the real response of the analyzed element, only if the considered element is similar to the ones in the data-base and that the numerical model is the same with that used to develop the fragility curves. The fragility curves developed herein have the advantage of being calibrated to experimental results so that the localization of the response due to numerical modeling is reduced. These curves can be used for models with the same numerical approximation if the obtained generalization is kept.

By using this kind of procedure, the intervention cost over a period of time can be estimated based on the expected damage measure. The damage measures presented are in general limit states that are observed for the materials of the reinforced concrete column, expressed as damage of concrete or reinforcement. The ductility or dissipated energy are not used as damage measures. The used damage measures can have associated intervention costs.

It was observed that each column will exhibit different limit states, according to its geometry, applied loads and material properties. A general model for drift isn't conservative to be applied. All these columns have different responses, so for assessing their vulnerability, each column should be analyzed. Extrapolating the results can be nonconservative and, in the case of columns that exhibit shear failure, physical unreliable.

Received on November 2, 2017

REFERENCES

1. BERRY, M.P., PARRISH, M., EBERHARD, M.O., *PEER Structural Performance Database, Version 1.0*, 2004.
2. BERRY, M.P., EBERHARD, M.O., *Performance modeling strategies for modern reinforced concrete bridge columns,* Technical Report 2007/07, PEER, April 2008.
3. CEANGU, V., *The influence of mathematical modeling of nonlinear behavior on the seismic response of civil constructions* (in Romanian), PhD Thesis, UTCB, November 2017.
4. CEB/FIP. *Model Code 2010.*
5. ELWOOD, K.J., MOEHLE, J.P.*, Shake table tests and analytical studies on the gravity load collapse of reinforced concrete frames,* Technical Report 2003/01, PEER, November 2003.
6. GALEOTA, D., GIAMMATTEO, M., MARINO, R.*, Strength and ductility of confined high strength concrete*, Proceedings of the Tenth World Conference on Earthquake Engineering, Madrid (Spain), Vol. 5, pp. 2609-2613, 1992.
7. JALAYER, F., CORNELL, C.A., *A technical framework for probability-based demand and capacity factor design (DCFD) seismic formats*, Technical Report PEER Report 2003/08, University of Berkeley, November 2003.
8. KOLOZVARI, K., ORAKCAL, K., WALLACE, J.*, Shear-flexure interaction modeling for reinforced concrete structural walls and columns under reversed cyclic loading*, Technical Report 2015/12, PEER, December 2015.

9. MANDER, J.B., PRIESTLEY, M.J.N., PARK, R*., Theoretical stress-strain model for confined concrete*, Journal of Structural Engineering, **114**, *8*, pp. 1804–1826, 1988.

10. MCGUIRE, R.K., *Seismic hazard and risk analysis*, EERI, MNO-10, 2004.

11. MCKENNA, F., FENVES. G.L., SCOTT, M.H., MAZZONI, S., *Open system for earthquake engineering simulation,* Technical report, PEER, June 2006.

12. SCOTT, M.H., HAMUTÇUOĞLU, O.M., *Numerically consistent regularization of force-based frame elements*, International Journal for Numerical Methods in Engineering, **76**, *1*, pp. 1612–1631, 2008.

13. SHOME, N., CORNELL, C.A., *Probabilistic seismic demand analysis of nonlinear structures*, Technical Report RMS-35, Stanford University, March 1999.

14. SPACONE, E., FILIPPOU, F.C., TAUCER, F., *Fibre beam-column model for non-linear analysis of R/C frames: Part I. Formulation*, Earthquake Engineering and Structural Dynamics, **25**, *1*, pp. 711–725, 1996.

15. VAMVATSIKOS, D., CORNELL, C.A., *Incremental dynamic analysis*, Earthquake Engineering and Structural Dynamics, **31**, *3*, pp. 491–514, 2002.

16. VĂCĂREANU, R., RADULIAN, M., IANCOVICI, M., PAVEL, F., NEAGU, C., *Fore-Arc and Back-Arc ground motion prediction model for Vrancea intermediate-depth seismic source*, Second European Conference in Earthquake Engineering and Seismology (2ECEES), Istanbul, Turkey, August 24-29, 2014..

17. ZHAO, J., SRITHARAN, S., *Modeling of strain penetration effects in fiber-based analysis of reinforced concrete structures*, ACI Structural Journal, **104**, *2*, pp. 133–141, 2007.